Desalination and Water Treatment
www.deswater.com
doi: 10.1080/19443994.2013.787028

52 (2014) 1484–1494
February

Taylor & Francis
Taylor & Francis Group

Bioadsorbtion of industrial dyes from aqueous solution onto water hyacinth (*Eichornia crassipes*): equilibrium, kinetic, and sorption mechanism study

Arijit Nath[a], Sudip Chakraborty[a,b], Chiranjib Bhattacharjee[a,*]

[a]*Chemical Engineering Department, Jadavpur University, Kolkata, West Bengal 700032, India*
Tel. +91 98364 02118; Fax: +91 33 2414 6203; email: cbhattacharyya@chemical.jdvu.ac.in
[b]*Department of Chemical Engineering and Materials, University of Calabria, 44/C, P. Bucci, Rende, CS 87036, Italy*

Received 3 December 2012; Accepted 12 March 2013

ABSTRACT

In the present investigation, bioadsorbtion of different industrial dyes, such as, methylene blue, Congo red, crystal violet, and malachite green from aqueous solution have been performed by water hyacinth using lab-scale batch bioreactor. Maximum removal of different dyes, such as, methylene blue, Congo red, crystal violet, and malachite green were found at pH 7.0, 6.0, 8.0, and 8.0, respectively. Optimum doses of adsorbent were found to be 6.5, 7.5, 6.0, and 7.0 g L^{-1} for methylene blue, Congo red, crystal violet, and malachite green, respectively. Optimum initial dyes concentration were found to be 65, 75, 70, and 75 mg L^{-1} for methylene blue, Congo red, crystal violet, and malachite green, respectively. Optimum contact time for adsorbtion was found to be 5 days for all the dyes. The maximum percentages of removals were found to be 90, 88, 92, and 90% for methylene blue, Congo red, crystal violet, and malachite green, respectively. The adsorption kinetic data are adequately fitted to the pseudo-second-order adsorption kinetic model. The Langmuir isotherm model well described the equilibrium dyes uptake. High value of intra particle diffusion parameter (K_i), and diffusion coefficient (D_i) suggest that water hyacinth is an effective adsorbent for the removal of industrial dyes from wastewater.

Keywords: Water hyacinth; Dyes; Parameters optimization; Adsorption kinetics; Equilibrium isotherm models; Sorption mechanism

1. Introduction

Dyes have become one of the main sources of severe water pollution as a result of rapid industrialization [1]. Different processing industries like textile, paper and pulp, rubber, cosmetic, and dyes producing industries discharge colored wastewater [2]. Presently, more than 10,000 different commercial dyes and pigments exist, and about 7×10^5 tons are produced annually worldwide [3]. The presence of very small amounts of dyes in water is highly visible and undesirable [4]. Effluent from dyes consuming industries creates the severe disposal problems because of toxic, carcinogenic, mutagenic, and teratogenic effects of dyes [5]. The dyes also disturb aquatic equilibrium, photosynthesis, as well as the food chain [6]. Therefore, treatment of effluent of dyes consuming industries attracts a great attention.

*Corresponding author.

Different process technologies, such as, reverse osmosis, flocculation, activated carbon adsorbtion, and microbial treatment have already been attempted for detoxification of dyes. The main disadvantage of the technology, proposed above, entail high operating cost, and therefore, those are not effectively used to treat the wide range of effluents. The bioadsorption is one of the effective methods for the removal of dyes from the textile wastewater [7]. At present, there is a growing interest of researchers in using other low-cost adsorbents for dyes removal. Many materials like coir pith [8], sun flower stalks [9], corn cobs and barley husk [10], rice husk [11], neem leaves [12], mango seed kernel [13], modified saw dust [14], giant duck weed [15], peanut hulls [16], pineapple stem [17], treated wood shavings [18], banana pith [19], orange peel [20], guava leaf [21], wheat shell [22] wheat bran [23], egg shell [24], natural Jordanian Tripoli [25], almond Shell (*Prunus dulcis*) [26], rubber wood (*Hevea brasiliensis*) sawdust [27], aqua cultural shell powders (prawn waste) [28], neem saw dust [29], degreased coffee bean [30], lemon peel [31], *Firmiana simplex* wood fiber [32], mango (*Mangifera indica* L.) seed husks [33], low-cost chlorella-based biomass [34], citric acid modified rice straw [35], groundnut shell waste based powdered activated carbon [36], and jute fiber carbon [37] have been used as a low cost absorbent for dye removal from aqueous system. However, as the adsorption capacities of the above mentioned adsorbents are not very satisfactory, still the searches for new bioadsorbents which are more eco-friendly, economic, easily available, and highly effective are continuing.

Water hyacinth (*Eichornia crassipes*) is a tropical and subtropical mycrophyte, whose appetite for nutrients has been put to use in cleaning up municipal, agricultural, industrial, and domestic wastewater. Water hyacinth is the faster multiplying weed, capable of doubling within a period of 12 to 15 days. On an average, it produces 200 tonnes of biomass for acre within a short period. Therefore, use of water hyacinth for detoxification of wastewater will boost up dyes consuming industries.

In the present research, bioadsorbtion is tested for simulated aqueous solution of methylene blue (methylthioninium chloride), Congo red (disodium 4-amino-3-[4-[4-(1-amino-4-sulfonato-naphthalen-2-yl)diazenylphenyl]phenyl]diazenyl-naphthalene-1-sulfonate), crystal violet (Tris (4-(dimethylamino)phenyl) methylium chloride) and malachite green (4-[(4-dimethylamin ophenyl)phenyl-methyl]-*N*,*N*-dimethylaniline) by water hyacinth in batch mode. A bench top reactor, 18 inch length, 12 inch width, and 2 inch depth and made by poly-ethylene was used for experimentation. Different process parameters, such as, pH of solution (2–10), doses of bioadsorbent (2–10 g L^{-1}), initial dye concentration (15–95 ppm), and adsorbtion time (1–7 days) were investigated. During the experiment, electric white light source (804.76 μw/cm^2 at 400 to 800 nm) was used as a photon source for promoting photosynthesis and experiment was performed at room temperature, 32°C ± 2. The adsorption kinetic models, equilibrium isotherm models, sorption mechanism, and parameters related with the process were investigated in detail.

2. Material and methods

2.1. Materials

Small amount of water hyacinth was collected from the local pond, near Jadavpur University, Kolkata, India. All the chemicals (analytical grade) were procured from Merk, Mumbai, India. The deionized water used in all the experiments was obtained from Arium 611DI ultrapure water system (Sartorius AG, Göttingen, Germany).

2.2. Equipment

An indigenous autoclave (G.B. Enterprise, Kolkata, India), an indigenous microfiltration unit along with cellulose acetate membrane of 47 mm diameter and 0.2 μm pore size (Sarada Chemicals, Kolkata, India), a hot air oven (Bhattacharya & Co., Kolkata, India), a magnetic stirrer, and an indigenous bench top reactor were used. The reactor, 18 inch length, 12 inch width, 2 inch depth and made by poly-ethylene was used for experimentation.

2.3. Analytical instruments

A digital pH meter, a digital weighing machine (Sartorius AG, Göttingen, Germany), a VARIAN UV–Visible spectrophotometer (Cary50 Bio) were used. Concentrations of Congo red (434 nm), methylene blue (650 nm), crystal violet (580 nm), and malachite green (620 nm) were estimated by colorimetric method using UV–VIS spectrophotometer.

2.4. Maintenance of water hyacinth

The roots of the collected water hyacinth were cleaned thoroughly with deionized water for several times to eliminate earthy matter and all the soil particles. The water hyacinth was cultivated at laboratory tub, 54 inch length, 36 inch width, 6 inch depth, and

made by poly-ethylene. Mineral solution, containing glucose 30 g, sodium chloride 10 g and dipotassium phosphate 10 g, and calcium carbonate 10 g/L was used as the cultivation medium for water hyacinth. The pH of the medium was adjusted at 7.0 by 0.1 N sodium hydroxide and 0.1 N hydrogen chloride. Sterilization of all components of the growth medium was done in an autoclave at 121 ℃ for 15 min. Glucose was sterilized using indigenous microfiltration unit equipped with cellulose acetate membrane (47 mm diameter, pore size-0.2 μm) for its sensitivity towards high temperature. The growth medium was changed at 7 days interval and electric white light source (804.76 μw/cm^2 at 400–800 nm) was used as a photon source for promoting photosynthesis. Water hyacinth was cultivated at room temperature, 32 ℃ ± 2.

2.5. Batch studies

Aqueous solution of different types of dyes such as, methylene blue, Congo red, crystal violet, and malachite green were used in present investigation. Several batch experiments were performed using an indigenous bench top reactor, made by poly-ethylene. Samples were withdrawn at 24 h interval, and each set of experiment was conducted for 7 days. Different process parameters, such as, pH of solution (2–10), doses of bioadsorbent (2–10 g L^{-1}), initial dye concentration (15–95 ppm), and contact time (1–7 days) were investigated. Initial pH of solution was adjusted at 7.0 by 0.1 N sodium hydroxide and 0.1 N hydrogen chloride. The amount of dye adsorbed per unit of water hyacinth (mg dye. per g water hyacinth) was calculated according to a mass balance on the dye concentration using Eq. (1),

$$q_e = \frac{(C_i - C_e)V}{m} \tag{1}$$

where q_e is the equilibrium dye concentration on adsorbent (mg g^{-1}), C_e represents equilibrium dye concentration in solution (mg L^{-1}), C_i is the Initial dye concentration (mg L^{-1}), m represents the mass of adsorbent (g), and V represents the volume of the solution. The percentage of removal of dye was calculated using the following equation:

$$\text{Removal } (\%) = \frac{(C_i - C_e)}{C_i} \times 100 \tag{2}$$

In order to ensure the reproducibility of the results, all the adsorption experiments were performed in triplicate, and the average values were used in data analysis. The error obtained was found to be within ± 3.0%.

3. Theoretical analysis

3.1. Adsorption isotherms

One of the objectives in this study was to determine the best fitted adsorbtion isotherm for dye adsorbtion on water hyacinth. To examine the relationship between the amount of the adsorbate adsorbed (q_e) to its concentration in the aqueous phase (C_e) at equilibrium, different isotherm models were widely employed for fitting the data. In the present investigation, the result of adsorption studies of different dyes onto a fixed amount of water hyacinth were fitted to models of Langmuir, Freundlich, Dubinin–Radushkevich (D–R), Redlich–Peterson (R–P), and Temkin equilibrium isotherm, and their goodness of fit were evaluated following vigorous statistical procedures.

3.1.1. Langmuir isotherm

The nonlinear form of the Langmuir equilibrium isotherm is

$$q_e = \frac{k_L \times q_m \times C_e}{1 + k_L \times C_e} \tag{3}$$

The linear form of the Langmuir equilibrium isotherm is

$$\frac{C_e}{q_e} = \frac{C_e}{q_m} + \frac{1}{k_L \times q_m} \tag{4}$$

The parameters of the Langmuir isotherm equilibrium model, namely maximum adsorption capacity of water hyacinth (q_m), (mg g^{-1}), and the Langmuir constant, (k_L), (L mg^{-1}) were evaluated by plotting C_e/q_e vs. C_e.

3.1.2. Freundlich isotherm

The nonlinear form of the Freundlich equilibrium isotherm is

$$q_e = k_F C_e^{1/n} \tag{5}$$

The linear form of the Freundlich equilibrium isotherm is

$$\log q_e = \log k_F + \left(\frac{1}{n}\right) \log C_e \tag{6}$$

The parameters of the Freundlich isotherm equilibrium model, namely the Freundlich constant, (k_F), ($mg\,g^{-1}$) ($L\,g^{-1}$)$^{1/n}$, and the Freundlich adsorption isotherm constant, n were evaluated by plotting log q_e vs. log C_e.

3.1.3. Dubinin–Radushkevich (D–R) isotherm

The nonlinear form of the Dubinin–Radushkevich (D–R) equilibrium isotherm is

$$q_e = q_m \times \exp(-\beta\varepsilon^2) \tag{7}$$

The linear form of the Dubinin–Radushkevich (D–R) equilibrium isotherm is

$$\ln q_e = \ln q_m - \beta\varepsilon^2 \tag{8}$$

The parameters of the Dubinin–Radushkevich (D–R) equilibrium isotherm model, namely maximum adsorption capacity of water hyacinth, (q_m), ($mg\,g^{-1}$), and the Dubinin–Radushkevich (D–R) equilibrium isotherm constant, β, ($mmol^2\,J^{-2}$), were evaluated by plotting lnq_e vs. ε^2. The Dubinin–Radushkevich (D–R) equilibrium isotherm model constant β gives an idea about the mean free energy of adsorption (E) and can be computed using the following relationship,

$$E = \frac{1}{\sqrt{2\beta}} \tag{9}$$

3.1.4. Redlich–Peterson (R–P) isotherm

The nonlinear form of the Redlich–Peterson (R–P) equilibrium isotherm is

$$q_e = \frac{k_R \times C_e}{1 + a_R \times C_e^{b_R}} \tag{10}$$

The linear form of the Redlich–Peterson (R–P) equilibrium isotherm is

$$\ln\left(\frac{k_R \times C_e}{q_e} - 1\right) = b_R \ln C_e + \ln a_R \tag{11}$$

The parameters of the Redlich–Peterson (R–P) equilibrium isotherm model, namely the Redlich–Peterson isotherm exponent, (b_R), the Redlich–Peterson (R–P) isotherm constant, k_R, ($L\,g^{-1}$), and the Redlich–Peterson (R–P) isotherm constant, a_R, ($L\,mmol^{-1}$)^{b_R} were evaluated by plotting C_e/q_e against $C_e^{b_R}$.

3.1.5. Temkin isotherm

The nonlinear form of the Temkin equilibrium isotherm is

$$q_e = \frac{RT}{b_T} \times \ln(A_T \times C_e) \tag{12}$$

The linear form of the Temkin equilibrium isotherm is

$$q_e = \frac{RT}{b_T} \times \ln A_T + \frac{RT}{b_T} \times \ln C_e \tag{13}$$

where T signifies absolute temperature, (°K), R represents universal gas constant, (8.314 J/mol°K). The parameters of Temkin equilibrium isotherm, namely the Temkin isotherm constant, A_t, ($L\,mmol^{-1}$), and another Temkin isotherm constant, b_T were evaluated by plotting q_e vs. ln C_e.

3.2. Adsorption kinetics

In order to analyze the adsorption kinetics of different dyes onto water hyacinth from aqueous solution, the pseudo-first-order and pseudo-second-order kinetic equations were applied to the experimental data.

From the first principle, the pseudo-first-order rate expression is followed by,

$$\frac{dq_t}{dt} = k_1(q_e - q_t) \tag{14}$$

where q_t represents amount of dye adsorbed at any time t ($mg\,g^{-1}$) by water hyacinth and k_1 is the pseudo-first-order rate constant (day^{-1}). The integral linear form of Eq. (14) is,

$$\log(q_e - q_t) = \log q_e - \frac{k_1}{2.303} \times t \tag{15}$$

Pseudo-first-order rate constant, k_1 is evaluated by plotting (q_e–q_t) vs. t.

Expression for the pseudo-second-order rate expression is followed by,

$$\frac{dq_t}{dt} = k_2(q_e - q_t)^2 \tag{16}$$

where k_2 was the pseudo-second-order rate constant ($g\,mg^{-1}\,day^{-1}$). The integral linear form of Eq. (16) is,

$$\frac{t}{q_t} = \frac{1}{k_2 \times q_e^2} - \frac{t}{q_e} \tag{17}$$

Pseudo-second-order rate constant, k_2 is evaluated by plotting (t/q) vs. t.

3.3. Sorption mechanism

Any adsorbtion process is done by either by physical nature (pore diffusion) or chemiadsorbtion mechanism. Under the investigation, it was assume that the process was done by intra-particle diffusion mechanism and an attempt was made to justify the assumption by real experimental result. According to Weber and Morris, an intra-particle diffusion coefficient, K_i is defined by,

$$K_i = q_t \times t^{-0.5} + I \tag{18}$$

The values of K_i ($\mathrm{mg\,g^{-1}\,day^{-1}}$) were determined for every 24 h intervals [38].

The kinetic data were further analyzed using the Boyd kinetic expression [39]. The Boyd kinetic expression is given by,

$$F = 1 - (6 \times \pi^{-2}) \exp(-\mathrm{Bt}) \tag{19}$$

and

$$F = q_t \times q_0^{-1} \tag{20}$$

where q_0 represents the amount of dye adsorbed at infinite time ($\mathrm{mg\,g^{-1}}$) onto water hyacinth, F represents the fraction of solute absorbed at time t, and Bt is a mathematical function of F. Substituting Eq. (20) in Eq. (19), it may be written that,

$$\mathrm{Bt} = -0.4977 - \ln(1 - F) \tag{21}$$

The Bt values at different contact times can be calculated using Eq. (20). The calculated B values were used to calculate the effective diffusion coefficient, D_i ($\mathrm{cm\,day^{-1}}$) using the following relation,

$$B = \prod^2 \times D_i \times r^{-2} \tag{22}$$

where r represents the radius of pore of adsorbent.

3.4. Statistical analysis

The accuracy of estimated above model parameters can be described by two methods.

Method 1: Determination of parameters through minimization of objective function including the sum of squared errors/deviations between the predicted and experimental values of concentrations of components under consideration.

Method 2: Determination of parameters through minimization of objective function including the sum of squared errors/differences between the predicted and experimental values of individual variables as obtained from batch experimental runs.

Since no literature data is available on the possible ranges of values of dye adsorbtion kinetic parameters for water hyacinth therefore, in the present case, method 2 has been adopted to determine the parameters. Regression analyses of data obtained from the parameter estimation experiments, described in theoretical analysis section have been done. For each regression analysis, the confidence intervals (R^2) have been determined.

3.4.1. Correlation coefficient

In order to estimate the strength of respective analysis, the coefficient of correlation has been determined. For any regression equation $y = a + bz$, the coefficient of correlation, r^* may be represented as follows [40,41].

$$r^* = b\sqrt{\frac{n\sum_{i=1}^{n} z_i^2 - \left(\sum_{i=1}^{n} z_i\right)^2}{n\sum_{i=1}^{n} y_i^2 - \left(\sum_{i=1}^{n} y_i\right)^2}} \tag{23}$$

where n = sample size, i = any value.

3.4.2. Confidence interval

The quality of parameter estimation is indicated by the confidence interval (R^2) [40,41]. Smaller interval means a high quality of parameter estimate or a smaller error.

A $100(1-\alpha)\%$ prediction interval on new observation is obtained using the following expression,

$$y_{\mathrm{obs}} = y_p \pm t_{\alpha/2,n-2}\sqrt{\mathrm{MS}_E\left[1 + \frac{1}{n} + \frac{(z_p - \bar{z})}{\sum_{i=1}^{n}(z_i - \bar{z})^2}\right]} \tag{24}$$

where MS_E = Error mean square

$$\mathrm{MS}_E = \mathrm{SSE}/\mathrm{dof}\ (\mathrm{SSE}) \tag{25}$$

where SSE = Sum of square of deviations between observed and predicted values of regressed variable used for parameter estimation

dof = Degree of freedom

To calculate the confidence interval (R^2) for any value, z_p of independent variable, the deviation between the observed value, y_{obs} and predicted regressed value, y_p of dependent variable was calculated. Using the value of the deviation and the value of $\sqrt{\mathrm{MS}_E\left[1+\frac{1}{n}+\frac{(z_p-\bar{z})}{\sum_{i=1}^{n}(z_p-\bar{z})^2}\right]}$, value of $\alpha/2$ is determined by consulting Student's t distribution table. Percent confidence interval (R^2) or prediction interval is given by $100(1-\alpha)$. At $x\%$ confidence interval, $\alpha = (100-x)/100$. The values of confidence intervals for regression equations involving model parameters have been determined using the new observations which are not utilized for parameter estimation (validation data).

4. Results and discussion

Different sets of batch experiments were conducted for individual dyes in batch mode using water hyacinth as a bioadsorbent. Aqueous solution of different types of dyes, such as, methylene blue, Congo red, crystal violet, and malachite green were used as adsorbet.

4.1. Effect of pH

The pH of an aqueous solution is an important monitoring parameter in dye adsorption, as it affects the surface charge of the adsorbent material and the degree of ionization of the dye molecule. It is also directly related with competition ability of hydrogen ions with the adsorbate molecules to active sites on the adsorbent surface. In Fig. 1, percentages of removal of different dyes from aqueous solution are plotted against different pH of solution. In this case, after 7 days of adsorption process aqueous solution were considered to study the effects of pH on bioadsorbtion. From Fig. 1, it is depicted that the percentages of removal of dyes by the water hyacinth increase with the increase in pH of the dye solution, appreciably up to pH 6.0. Maximum removal of different dyes, such as, methylene blue, Congo red, crystal violet, and malachite green were found at pH 7.0, 6.0, 8.0, and 8.0, respectively. After the critical values of solution pH, the values of percentage removal were remain unchanged. Water hyacinth root mainly contains $-PO_4$, C=O and C–H functional groups at their surface and all the dyes are cationic charged, which exists in aqueous solution in the form of positively charged ions. At low pH values, protonation of the functional groups present on the adsorbent surface easily takes place. The surface of the adsorbent

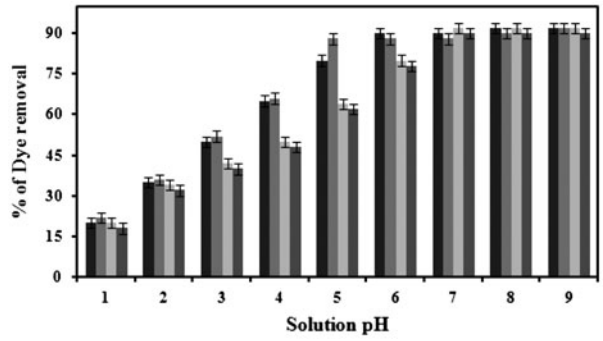

Fig. 1. Effect of solution pH on different dyes adsorbtion onto water hyachinth. ■ Methylene blue, ■ Congo red, ■ crystal violet, ■ malachite green.

becomes positively charged, and this decreases the adsorption of the positively charged dye ions through electrostatic repulsion. However, as the pH of the dye solution increases, a considerable increase in dye binding capacity is observed due to strong electrostatic attraction between negatively charged sites on the biosorbent and the dye cations. Similar type of observation was found by Chakraborty et al., for batch removal of crystal violet from aqueous solution by H_2SO_4 modified sugarcane bagasse [1].

4.2. Effect of adsorbent doses

Adsorbent doses have a significant influence on the adsorption process. In Fig. 2, percentages of different dyes removal are plotted against different doses of adsorbent at critical pH of individual dyes. In this case, concentrations of individual dyes were maintained $70\,\mathrm{mg\,L^{-1}}$. From the figure, it is depicted that the percentage of dye removal increases with the increase of biosorbent dose from 2 to $6\,\mathrm{g\,L^{-1}}$. It may

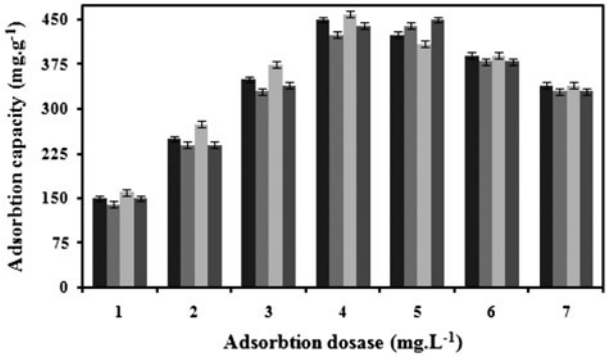

Fig. 2. Effect of adsorbent doses on different dyes adsorbtion onto water hyachinth. ■ Methylene blue, ■ Congo red, ■ crystal violet, ■ malachite green.

be justified by the fact that the increase in the percentage of dye removal with the adsorbent dose could be attributed to an increase in the adsorbent surface area, augmenting the number of adsorption sites and porous channel available for adsorption. However, the decrease in sorption capacity with the increasing adsorbent dose at constant dye concentration and volume may be attributed to saturation of sorption sites due to particulate interaction such as aggregation. Such aggregation would lead to a decrease in the total surface area of the adsorbent.

4.3. Effect of initial dye concentration

For an effective adsorption, the initial concentrations of the adsorbate are an important factor. In Fig. 3, adsorbtion capacities ($mg\,g^{-1}$) are plotted against different initial concentrations of dyes. In this case, concentration of adsorbent was maintained $8\,g\,L^{-1}$. From the figure, it is depicted that the adsorption capacity of water hyacinth is increased with the increase of initial dye concentration at a certain level, after that the process is almost saturated. The increase in dye uptake capacity can be justified by the fact that increasing concentrations gradient of dyes provide an increasing driving force to overcome all mass transfer resistances of the dye molecules between the aqueous and solid phase, leading to an increased equilibrium uptake capacity until sorbent saturation is achieved. On the contrary, the percentages removal of dyes decreases with the increase in initial dye concentration. This can be explained by the fact that all adsorbents have a limited number of active sites and porous channel, which become saturated at a certain concentrations of dyes. Optimum initial dyes concentration were found 65, 75, 70, and $75\,mg\,L^{-1}$ for methylene blue, Congo red, crystal violet, and malachite green, respectively.

4.4. Effect of adsrbtion time

In Fig. 4, time histories of percentages of dye removals are plotted against different adsorbtion time at critical pH, initial dye concentration, and doses of bioadsorbent for individual dyes. It is observed that maximum dyes are removed in 5 day. The maximum percentages of removal were fond 90, 88, 92, and 90% for methylene blue, Congo red, crystal violet, and malachite green, respectively. This is justified by the fact that almost active site and porous channel of adsorbent are saturated by dye molecules at a certain period of adsorbtion. The batch type of bioadsorbtion experiment was conducted at only dye solution under different physicochemical parameters whereas, maintenance medium of water hyacinth is chemically defined medium. We cannot found any type of significant change of proposed mycrophyte within this short time (7 days) of batch experiment.

4.5. Equilibrium isotherm

4.5.1. Model parameters

The different isotherm model equations used in the present investigation contain a large number of parameters, whose values have been experimentally found out. In Table 1, the magnitudes of estimated parameters of different isotherm models (Eqs. 3–13) are described along with confidence intervals (R^2) for different dyes. For all evaluated model parameters, the confidence intervals are checked for new observations of respective experiments dedicated to the evaluation of parameters. New observations are independent of those used to obtain the values of model parameters through the regression analysis.

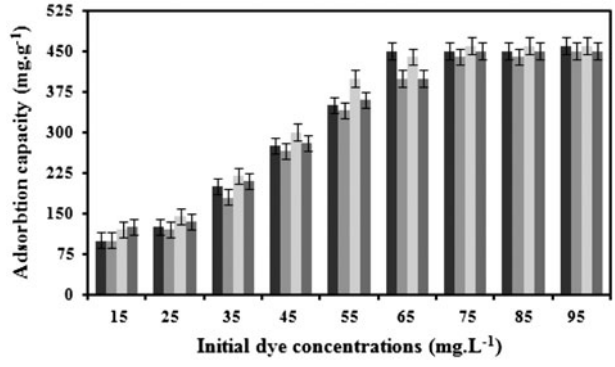

Fig. 3. Effect of initial dyes concentrations on bioadsorbtion process by water hyachinth. Methylene blue, Congo red, crystal violet, malachite green.

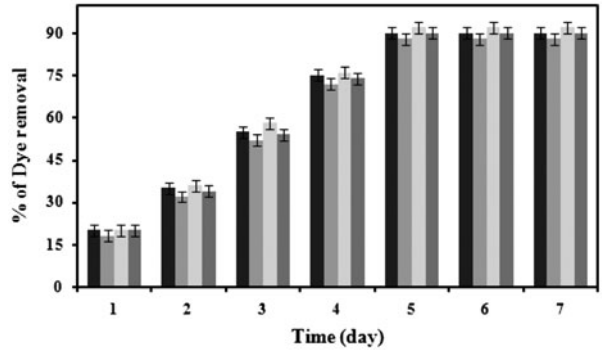

Fig. 4. Time histories of dyes adsorbtion onto water hyachinth. Methylene blue, Congo red, crystal violet, malachite green.

Table 1
Isotherm constants and % confidence intervals and correlation coefficient for model fits of bioadsorption of dyes onto water hyacinth at optimum operating conditions for methylene blue, Congo red, crystal violet and malachite green

Langmuir isotherm	q_m (mg g^{-1})	k_L (L mg^{-1})	Corelation coefficient	Confidence interval (%)
Methylene blue	148	1.8	0.999	99.9
Congo red	149	1.79	0.999	99.8
Crystal violet	150	1.8	0.999	99
Malachite green	148	1.82	0.999	98
Freundlich isotherm	k_F (mg g^{-1}). (L mg^{-1})$^{1/n}$	n		
Methylene blue	32	2.46	0.86	86
Congo red	30	2.45	0.87	87
Crystal violet	29	2.44	0.88	88
Malachite green	30	2.45	0.88	88
Dubinin–Radushkevich (D–R) isotherm	β (mmol^2 J^{-2})	E (kJ mol^{-2})		
Methylene blue	5.3×10^{-9}	11.46	0.96	96
Congo red	5.29×10^{-9}	11.45	0.95	95
Crystal violet	5.28×10^{-9}	11.47	0.97	98
Malachite green	5.28×10^{-9}	11.45	0.96	97
Redlich–Peterson (R–P) isotherm	k_R (L g^{-1})	b_R		
Methylene blue	0.54	0.3	0.9	89
Congo red	0.56	0.301	0.92	92
Crystal violet	0.55	0.302	0.9	90
Malachite green	0.55	0.302	0.92	92
Temkin isotherm	b_t	A_t (L mmol^{-1})		
Methylene blue	69,015	1.68	0.96	96
Congo red	69,018	1.72	0.95	95
Crystal violet	69,014	1.7	0.95	95
Malachite green	69,014	1.7	0.96	96

4.5.2. Estimation of model fits for lab scale reactor

The accuracy and confidence level of the proposed model equations have been evaluated by the mean squared error (MS_E) criterion and Fisher's F ratio test [41].

$$F \text{ ratio} = \frac{MS_R}{MS_E} \tag{26}$$

where $MS_R = \frac{SSR}{dof}$, dof = 1

$$SSR = \sum \left(y_{pi} - \bar{y}\right)^2 \tag{27}$$

$$MS_E = \frac{\left(y_{obs_i} - y_{p_i}\right)^2}{dof} \tag{28}$$

$$dof = n - m \tag{29}$$

m = number of constants involved in model equations.

The significance level, p, is determined from the value of F, dof of quantity in the numerator, i.e. 1 and

Table 2
Statistical evaluation of the fits of different isotherm models to the measurements

Isotherm models	MS_E	Confidence level α (From Fisher F test)	% $100(1-\alpha)$
Langmuir	1.9354×10^{-7}	0.001	99.9
Freundlich	4.25×10^{-5}	0.08	92
Dubinin–Radushkevich (D–R)	5.45×10^{-3}	0.05	95
Redlich–Peterson (R–P)	5.55×10^{-3}	0.045	95.5
Temkin	5.55×10^{-4}	0.055	94.5

dof of the quantity in the denominator, i.e. $(n-m)$. Evaluation of such confidence level and accuracies of model equations (usually referred to as the strength of the mathematical model) using the statistical approach has been done [25,26]. The experimental results, shown in Table 2, indicate that adsorbtion of different types of dyes onto water hyacinth follows the Langmuir isotherm model mostly, compared to other isotherm models. The suitability of the Langmuir isotherm model suggests monolayer coverage of dye molecules on the biosorbent surface. Each molecule has equal activation energy and that sorbate–sorbate interaction is negligible. The value of the Freundlich constant n is significantly higher for all the pH value studied, indicate that the dyes biosorption behavior of water hyacinth can be considered as favorable. The Dubinin–Radushkevich (D–R) isotherm model constant β gives an idea about the mean free energy, E ($kJ\,mol^{-1}$) of adsorption per mole of the adsorbate which in turn can give information about the type of sorption mechanism. The estimated values of E for methylene blue, Congo red, crystal violet, and malachite green were found to be 7, 7.2, 6.8, and $7\,kJ\,mol^{-1}$, respectively at proposed experiment, which implies that the biosorption mechanism of dyes on water hyacinth involves physical nature instead of chemisorption. In case of the Redrich–Peterson (R–P) isotherm model, the values of confidence intervals (R^2) are not significantly high, which also signify that the process is physical adsorbtion instead of ion exchange. High A_t value of Temkin model reveals that, heat of adsorption of all the molecules in layer decreases linearly with coverage due to adsorbent–adsorbate interactions, and that the adsorption is characterized by a uniform distribution of the bonding energies, up to some maximum binding energy.

4.6. Evaluation of adsorbtion kinetics

The values of different rate constants of sorption kinetic model along with confidence intervals (R^2) are described in Table 3. From this analysis, it is depicted that adsorption of different dyes onto water hyacinth does not follow pseudo-first-order kinetics. The kinetic data showed the excellent fit to the pseudo-second-order kinetic equation at all pH values.

4.7. Sorption mechanism

During batch mode of operation, there is a possibility of intra-particle pore diffusion of adsorbate ions, which can be the rate-limiting step. Therefore, the possibility of the intra-particle diffusion resistance affecting the adsorption process was explored by using the intra-particle diffusion model. According to Eq. (18), a plot of q_t vs. $t^{0.5}$ should be a straight line with a slope K_i, intra-particle diffusion parameter and intercept I, which signifies that the adsorption mechanism follows the intra-particle diffusion process (figure not shown). In Fig. 5, intra-particle diffusion coefficient, K_i is plotted against individual initial dyes

Table 3
Sorption kinetic constant and confidence intervals (R^2) of dye adsorbtion process onto water hyacinth

	Pseudo-first-order		Pseudo-second-order	
	k_1 (min^{-1})	R^2	k_2 ($g\,mg^{-1}\,min^{-1}$)	R^2
Methylene blue	1.82×10^{-3}	0.65	2.32×10^{-3}	0.99
Congo red	2.52×10^{-3}	0.52	1.52×10^{-3}	0.98
Crystal violet	2.45×10^{-3}	0.42	3.22×10^{-3}	0.99
Malachite green	2.25×10^{-3}	0.58	1.85×10^{-3}	0.97

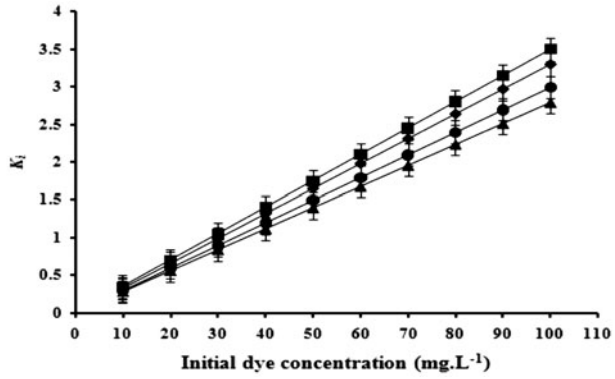

Fig. 5. Intra-particle diffusion coefficient, K_i against different initial concentrations of individual dyes. ◆ Methylene blue, ■ Congo red, ▲ crystal violet, ● malachite green.

concentrations. A linear co-relation, as a result of plotting K_i against different initial dyes concentrations also suggests the pore diffusion assumption. This result is also supported by the Boyd kinetic expression. High value of diffusion coefficient (D_i) also supports the pore diffusion mechanism during bioadsorbtion (data not shown).

From the above experimental findings it may be proposed that water hyacinth is potential for detoxification of wastewater of dyes consuming industries. This kinetic model may be used to predict the behavior of different types of bioreactor configurations, including variations of operating parameters for the process of bioadsorbtion at real situation.

Conclusions

By a batch adsorbtion process different process parameters were optimized. Those are highlighted below.

(1) Optimum pH of different dyes, such as, methylene blue, Congo red, crystal violet, and malachite green were 7.0, 6.0, 8.0, and 8.0, respectively.
(2) Optimum doses of adsorbent were found to be 6.5, 7.5, 6.0 and, 7.0 g L^{-1} for methylene blue, Congo red, crystal violet, and malachite green, respectively.
(3) Optimum initial dyes concentration were found to be 65, 75, 70 and, 75 mg L^{-1} for methylene blue, Congo red, crystal violet, and malachite green, respectively.
(4) Optimum contact time for adsorbtion was found to be 5 days for all of the dyes.
(5) The maximum percentages of removals are found to be 90, 88, 92, and 90% for methylene blue, Congo red, crystal violet, and malachite green, respectively.

The adsorption kinetic data are adequately fitted to the pseudo-second-order adsorption kinetic model. The Langmuir isotherm model well described the equilibrium dye uptake. This signifies that adsorbtion of organic dyes onto water hyacinth is done by monolayer formation. High value of intra-particle diffusion parameter (K_i), and diffusion coefficient (D_i) suggest the pore diffusion mechanism during bioadsorbtion. Therefore, it may be concluded that the proposed methodology is an effective route of wastewater treatment of dyes consuming industries.

Acknowledgments

CSIR is greatly acknowledged for providing scholarship to first author as SRF. The authors gratefully acknowledge the financial support (vide sanction letter no. DST/TMC/2K11/345 dated 17.05.2012) provided by Department of Science and Technology (DST, India) for the New INDIGO project entitled "From Grey to Green: How to Improve the Sustainability of Wastewater and Drinking Water".

References

[1] S. Chakraborty, S. Chowdhury, P. Das Saha, Batch removal of crystal violet from aqueous solution by H_2SO_4 modified sugarcane bagasse: Equilibrium, kinetic, and thermodynamic profile, Sep. Sci. Technol. 47 (2012) 1898–1905.
[2] G. McKay, J.F. Porter, G.R. Prasad, The removal of dye colors from aqueous solutions by adsorption on low-cost materials, Water Air Soil Pollut. 114 (1999) 423–438.
[3] C.I. Pearce, J.R. Lloyd, J.T. Guthrie, The removal of colour from textile wastewater using whole bacterial cells: A review, Dyes Pigm. 58 (2003) 179–196.
[4] T. Robinson, G. McMullan, R. Marchant, P. Nigam, Remediation of dyes in textile effluent: A critical review on current treatment technologies with a proposed alternative, Bioresour. Technol. 77 (2001) 247–255.
[5] D. Ghosh, K.G. Bhattacharyya, Adsorption of methylene blue on kaolinite, Appl. Clay Sci. 20 (2002) 295–300.
[6] A. Ozer, G. Dursun, Removal of methylene blue from aqueous solution by dehydrated wheat bran carbon, J. Hazard. Mater. 146 (2007) 262–269.
[7] K.S. Low, C.K. Lee, K.K. Tan, Bioadsorption of basic dye by *Eichhornia crassipes* roots, Bioresour. Technol. 52 (1995) 79–83.
[8] C. Namasivayam, K. Kadirvelu, Coir pith as an agricultural waste byproduct for the treatment of dyeing wastewater, Bioresour. Technol. 48 (1994) 79–81.
[9] G. Sun, X. Xu, Sunflower stalks as adsorbents for color removal from textile wastewater, Ind. Eng. Chem. Res. 36 (1997) 808–812.
[10] B. Chandran, P. Nigam, Removal of dyes from an artificial textile dye effluent by two agricultural waste residues, corncob and barley husk, Environ. Int. 28 (2002) 29–33.

[11] S. Chowdhury, P. Saha, Adsorption kinetic modeling of safranin onto rice husk biomatrix using pseudo-first- and pseudo-second-order kinetic models: Comparison of linear and non-linear methods, Clean—Soil, Air, Water 39 (2011) 274–282.
[12] K.G. Bhattacharyya, A. Sharma, Kinetics and thermodynamics of methylene blue adsorption on neem (*Azadirachta indica*) leaf powder, Dyes Pigm. 65 (2005) 51–59.
[13] K.V. Kumar, A. Kumaran, Removal of methylene blue by mango seed kernel powder, Biochem. Eng. J. 27 (2005) 83–93.
[14] D.S. De, J.K. Basu, Adsorption of methylene blue onto a low cost adsorbent developed from sawdust, Indian J. Environ. Prot. 19 (1998) 416–421.
[15] P. Waranusantigul, P. Pokethitiyook, M. Kruatrachue, E.S. Upatham, Kinetics of basic dye (methylene blue) biosorption by giant duckweed (*Spirodela polyrrhiza*), Environ. Pollut. 125 (2003) 385–392.
[16] S.J. Allen, Q. Gan, R. Matthews, P.A. Johnson, Mass transfer processes in the adsorption of basic dyes by peanut hulls, Ind. Eng. Chem. Res. 44 (2005) 1942–1949.
[17] S. Chakraborty, S. Chowdhury, P. Das Saha, Insight into biosorption equilibrium, kinetics and thermodynamics of crystal violet onto *Ananas comosus* (pineapple) leaf powder, Appl. Water Sci. 2 (2012) 135–141.
[18] P. Janos, S. Coskun, V. Pilarova, J. Rejnek, Removal of basic (methylene blue) and acid (egacid orange) dyes from waters by sorption on chemically treated wood shavings, Bioresour. Technol. 100 (2008) 1450–1453.
[19] C. Namasivayam, D. Prabha, M. Kumutha, Removal of dyes by adsorption on to agricultural solid waste, Bioresour. Technol. 62 (1997) 123–127.
[20] R. Sivaraj, C. Namasivayam, K. Kadirvelu, Orange peel as an adsorbent in the removal of acid violet 17 (acid dye) from aqueous solution, Waste Manage. 21 (2001) 105–110.
[21] V. Ponnusami, S. Vikram, V. Srivastava, Guava (*Psidium guajava*) leaf powder: Novel adsorbent for removal of methylene blue from aqueous solutions, J. Hazard. Mater. 152 (2008) 276–286.
[22] Y. Bulut, H. Aydın, A kinetics and thermodynamics study of methylene blue adsorption on wheat shells, Desalination 194 (2006) 259–267.
[23] O. Hamdaoui, M. Chiha, Removal of methylene blue from aqueous solutions by wheat bran, Acta. Chim. Slov. 54 (2007) 407–418.
[24] S. Chowdhury, S. Chakraborty, P. Das Saha, Removal of crystal violet from aqueous solution by adsorption onto eggshells: Equilibrium, kinetics, thermodynamics and artificial neural network modeling, Waste Biomass Valor. (2012). 1–10 doi: 10.1007/s12649-012-9139-1
[25] A.S. Alzaydien, Adsorption of methylene blue from aqueous solution onto a low cost natural Jordanian Tripoli, Am. J. Environ. Sci. 5 (2009) 197–208.
[26] D. Ozdes, A. Gundogdu, C. Duran, H.B. Senturk, Evaluation of adsorption characteristics of malachite green onto almond shell (*Prunus dulcis*), Sep. Sci. Technol. 45 (2010) 2076–2085.
[27] K.V. Kumar, S. Sivanesan, Isotherms for malachite green onto rubber wood (*Hevea brasiliensis*) sawdust: Comparison of linear and non-linear methods, Dyes Pigm. 72 (2007) 124–129.
[28] T. Santhi, S. Manonmani, T. Smitha, K. Mahalakshmi, Adsorption of malachite green from aqueous solution onto a waste aqua cultural shell powders (prawn waste): Kinetic study, Rasayan J. Chem. 2 (2009) 813–824.
[29] S.D. Khattri, M.K. Singh, Removal of malachite green from dye wastewater using neem sawdust by adsorption, J. Hazard. Mater. 167 (2009) 1089–1094.
[30] M.H. Baek, C.O. Ijagbemi, O. Se-Jin, D.S. Kim, Removal of malachite green from aqueous solution using degreased coffee bean, J. Hazard. Mater. 176 (2010) 820–828.
[31] K.V. Kumar, Optimum sorption isotherm by linear and non-linear methods for malachite green onto lemon peel, Dyes Pigm. 74 (2007) 595–597.
[32] X. Pan, D. Zhang, Removal of malachite green from water by *Firmiana simplex* wood fiber, Electron. J. Biotechnol. 12 (2009) 1–10.
[33] A.S. Franca, L.S. Oliveira, S.A. Saldanha, P.I.A. Santos, S.S. Salum, Malachite green adsorption by mango (*Mangifera indica* L.) seed husks: Kinetic, equilibrium and thermodynamic studies, Desalin. Water Treat. 19 (2010) 241–248.
[34] W.T. Tsai, H.R. Chen, Removal of malachite green from aqueous solution using low-cost chlorella-based biomass, J. Hazard. Mater. 175 (2010) 844–849.
[35] R. Gong, Y. Jin, F. Chen, J. Chen, Z. Liu, Enhanced malachite green removal from aqueous solution by citric acid modified rice straw, J. Hazard. Mater. B137 (2006) 865–870.
[36] R. Malik, D.S. Ramteke, S.R. Wate, Adsorption of malachite green on groundnut shell waste based powdered activated carbon, Waste Manage. 27 (2007) 1129–1138.
[37] K. Porkodi, K.V. Kumar, Equilibrium, kinetics and mechanism modeling and simulation of basic and acid dyes sorption onto jute fiber carbon: Eosin yellow, malachite green and crystal violet single component systems, J. Hazard. Mater. 143 (2007) 311–327.
[38] W.J. Weber, J.C. Morris, Kinetics of adsorption on carbon from solution, J. Sanit. Eng. Div. Am. Soc. Civ. Eng. 89 (1963) 31–60.
[39] G.E. Boyd, A.W. Adamson, L.S. Myers, Jr. The exchange adsorption of ions from aqueous solutions by organic zeolites. II. Kinetics, J. Am. Chem. Soc. 69 (1947) 2836–2848.
[40] V. Kafarov, Cybernatic Methods in Chemistry & Chemical Engineering (B. Kuzetson, Trans.), second ed., Mir, Moscow, 1976.
[41] A. Constantinides, Applied Numerical Methods with Personal Computers (Chemical Engineering Series), first ed., McGraw-Hill International Editions, New York, NY, 1987.